JOURNAL OF MATERIALS SCIENCE 32 (1997) 3497–3502

Finite-element modelling of crack propagation in elastic–plastic media

Part II *Horizontal subsurface cracks*

K. SADEGHIPOUR, G. BARAN*, Z. FU and S. JAYARAMAN
*Department of Mechanical Engineering and *School of Dentistry, Temple University, Philadelphia, PA, USA*

Horizontal subsurface cracks in an elastic–plastic material are analysed using finite-element techniques. The sliding surface is modelled as a rigid cylinder. The effect of such parameters as the friction between the cylinder and the material being indented, the elastic and plastic modulus of the material and the depth of crack location on the *J*-integral values at the left and right tips of a horizontal subsurface crack is considered. The prospective crack propagation direction is taken as the direction along which the *J* integral assumes a maximum as the indenter slides along the material surface. The left and right tip cracks were found likely to propagate at about 10° to the horizontal. This propagation direction was found to depend strongly on the location of the crack. Both crack tips are expected to propagate closer to the vertical direction as the depth of crack location is reduced. Also, horizontal cracks closer to the surface are found to have higher *J* integral values. While friction between the slider and the specimen did not affect the crack propagation direction, the crack-tip plasticity reduced the propagation direction, with respect to the horizontal.

1. Introduction

Understanding the material parameters contributing to the wear of polymers and polymer-based composites is of particular importance. These materials are being increasingly used as replacements for metal parts subject to sliding wear, in applications as diverse as machinery [1], dental prostheses [2] and orthopaedic prostheses [3]. Polymers are rather unique in that their material properties exhibit a great range depending on external conditions, particularly temperature. The strain rate also plays a role in determining material response [4]. It is therefore often not clear when linear elastic fracture mechanics (LEFM) may safely be used to describe crack propagation in polymers.

Much work has been done since the pioneering work of Suh [5] and Fleming and Suh [6] in attempting to relate the mechanisms of delamination and crack propagation to wear rates. Fracture mechanics have since been used to elucidate the problem of delamination theory of wear. Notable studies following that of Suh are those of Rosenfield [7] and Hills and Ashelby [8]. Keer *et al.* [9] have presented numerical results for a cracked surface loaded by Hertzian contact stresses. Ghosn [10] has analysed vertical surface crack propagation in a rotating inner raceway of a high-speed roller bearing using the boundary integral method. He has attempted to predict the crack growth direction of a vertical surface crack under rolling sliding contact. Recently, Salehizadeh and Saka [11] have calculated the stress intensity factors for short straight and branched subsurface cracks, subject to Hertzian loading, using the finite-element method. Their results were consistent with the earlier work of Fleming and Suh [6] in emphasizing the importance of mode II in crack propagation

Caution has to be exercised in using linear elastic fracture mechanics to understand these wear mechanisms. As pointed out by Rosenfield [12], when the crack tip is very close to a free surface, even usually brittle materials act as though they are tough. This led him to conclude that the formation of wear debris by growth of subsurface cracks is either *J* controlled or strength controlled. Also, as mentioned by Sin and Suh [13], a major shortcoming of some earlier contributions is the use of LEFM, even when the actual plastic zone adjacent to the crack tip is large and extends to the nearest free surface. When LEFM are used to predict the rate of crack propagation under cyclic loading, two conditions need to be satisfied. Firstly, the change, ΔK, in stress intensity factor should be larger than a critical value called the threshold value, ΔK_{th}. Secondly, the plastic zone size ahead of the crack tip is small compared with the dimensions of the crack or the distance of the crack tip from the nearest free surface.

Three criteria, namely, maximum hoop stress [14], minimum strain energy density [15], and maximum shear stress, are commonly used in predicting crack

0022–2461

propagation directions under single- or mixed-mode loading. The minimum-energy-density criterion, however, cannot be applied with confidence unless the plastic stress components are proportional to the corresponding elastic stress components, as these are based on elastic solutions. Also, these criteria cannot be used to explain crack propagation when cracks are under compressive and shear loading. Recently, Tikare and Choi [16] have tried to correlate the crack propagation direction of monolithic ceramics with the ratio of mode I to mode II stress intensity.

In the case of subsurface horizontal cracks, Suh proposed that the maximum-shear-stress criterion can be used to find the crack propagation direction. His proposal was based on the experimental findings of Jahanmir *et al.* [17], who showed firstly that subsurface cracks propagate parallel to the surface for a considerable distance before they change the direction and secondly that slip planes are shown to line up parallel to the surface in sliding wear. Fatigue experiments on steel samples under pure mode II loading conditions by Otsuka *et al.* [18, 19] indicate that at low values of mode II stress intensity factors the crack growth was along the direction of maximum shear stress, which happens to be in the direction of the crack line. At high mode II stress intensity factors the cracks branched at $\pm 70^\circ$ from the crack line. These angles correspond to the directions of maximum tensile hoop stress at the crack tip.

In sliding wear, several aspects of crack propagation need to be considered. Specifically these are, firstly the location of the moving load with respect to the crack tip, secondly the prospective crack propagation direction, and thirdly such factors as crack depth, crack face friction and crack geometry.

In the present study, a finite-element model is used to study horizontal subsurface cracks as a preliminary step to proposing a predictive wear model. The purpose is to simulate the cusp of an opposing tooth sliding over a restorative material surface during chewing. As a first approximation, the restorative material surface is assumed to be smooth, and the opposing cusp is modelled as a cylinder with radius R, allowing a simpler two-dimensional plane strain model to be employed. The interest is specifically in a polymer material, such as an epoxy-type thermoset.

Our scope here is rather modest. The results of previous work by Sadeghipour *et al.* [20] on static microindentation (specifically material modelling and the location and formation of different cracks) have been used for a sliding cylinder, when a subsurface horizontal crack exists. The effect of neighbouring subsurface cracks is ignored. It is the purpose of this study to use this simple model to predict the crack propagation direction of such cracks using the J-integral approach.

2. Theoretical background

The basic principles derived from static indentation fracture theory are still useful for understanding crack initiation and propagation in wear testing, even though the existence of a crack and the motion of the indenter sliding on the material surface affects the stress distribution patterns.

The constitutive model for the specimen material is based on a series of experimental microindentation tests reported in our previous publication [20]. Material response was simplified to be similar to a bilinear elastic–plastic von Mises material. As an indenter contacts the surface, the applied load is distributed over the contact site as compressive stresses. Elastic deformation of the material, both at and around the contact site, gives rise to tensile stresses confined to a shallow "skin" outside this region and compressive stresses immediately below. The combination of tensile and compressive stresses causes the formation of ring, median and radial cracks when spherical indenters were considered [20].

During the initial penetration, the stress field is usually described by three components: stresses radiating from the point of contact (radial stresses), stresses which encircle the contact (hoop stressed), and shear stresses. It is the behaviour of these stresses in the immediate vicinity of the contact (the so-called "near-field" stresses) which determine the point of initiation of indentation-induced cracks. Stresses at points far removed from the contact (the "far-field" stresses) also determine the path of propagation of the same cracks. All analyses were performed using the existing package ADINA 6.1 [21]. ADINA was chosen because of its capabilities of plastic analysis, contact mechanics analysis and fracture mechanics analysis.

In previous studies, the stress intensity factors, K_{I}, K_{II} and K_{III}, were usually chosen to describe the fracture behaviour in elastic fields. It is indeed the use of the stress intensity factor as the characterizing parameter for crack extension that is a fundamental principle of LEFM. However, the elastic distribution in the vicinity of a crack tip causes a stress singularity at the crack tip; thus the elastic solution is not unconditionally applicable.

The J integral is a generally accepted parameter to describe fracture behaviour in an elastic–plastic field. It is defined as

$$J = \int_{\Gamma} \left(W \, \mathrm{d}x_2 - \sigma_{ij} \frac{\partial u_i}{\partial x_i} n_j \, \mathrm{d}s \right) \qquad (1)$$

where Γ is the line contour enclosing the crack tip, x_i are Cartesian coordinates, σ_{ij} are the components of the stress tensor, u_i are the components of the displacement vector, n_j are the components of unit vector normal to Γ, $\mathrm{d}s$ is the length of the increment along Γ and $W = \int \sigma_{ij} \, \mathrm{d}\varepsilon_{ij}$ is the total stress work density (per unit volume). For linear elastic materials, J is related to the stress intensity factors as

$$J = \frac{K_{\mathrm{I}}^2}{E'} + \frac{K_{\mathrm{II}}^2}{E'} + \frac{K_{\mathrm{III}}^2}{G} \qquad (2)$$

where $E' = E$ in plane stress and $E' = E/(1-\nu^2)$ in plane strain.

In the present investigation, the "line contour" method is used to determine the cylinder location when crack initiation could occur [21]. This method is

used in a two-dimensional analysis to calculate the J integral, a contour-independent parameter characterizing the severity of the displacement, and the stress and strain field at the tip of the crack. When used in conjunction with finite-element models, the line contour is defined by a series of adjoining segments passing through the elements located on the contour. The integration of the J integral along each segment is performed numerically using the value of the variables at the integration points which define the segment.

According to the principles of fracture mechanics, all stress systems in the vicinity of a crack tip may be derived from three modes of loading, i.e., opening mode, sliding mode and tearing mode. The line contour method can reflect a realistic composition of those three modes because it is not necessary to verify a virtual displacement of a domain around the crack tip against a virtual extension method.

In contrast, the "virtual crack extension" method can only be used to determine the possible crack propagation direction. In this method, a small domain around a crack tip and its virtual possible extension direction must be specified *a priori*. This virtual extension direction is not always true during cylinder sliding from one side of the crack to the other, but it is true when the cylinder reaches a location at which the J integral has a maximum value. In other words, when a cylinder slides on a specimen surface, different potential crack propagation directions exist depending on the cylinder location. Further, there is a most likely crack propagation direction for each cylinder location. Therefore, this method can be used to evaluate the J integral of a given body with pre-existing cracks.

The total potential energy variation is calculated using a "virtual material shift" obtained by shifting the nodes of a domain which includes at least one of the crack's front nodes. The equivalence between the J integral and the ratio of the total potential energy variation to the crack area increase holds only for linear elastic and elastic–plastic analyses when the deformation theory of plasticity is applicable.

The equation for the energy release rate is expressed as

$$G = \frac{1}{A_c}\int_v \left[\left(\sigma_{ij}\frac{\partial u_j}{x_k} - W\delta_{ik}\right)\frac{\partial(\Delta x_k)}{\partial x_i} - f_i\frac{\partial u_i}{\partial x_j}\Delta x_j\right]\mathrm{d}v - \frac{1}{A_c}\int_s t_i\frac{\partial u_i}{\partial x_j}\Delta x_j\,\mathrm{d}s \quad (3)$$

where v is the volume of the cracked body, s is the surface of the cracked body, Δx_k are the components of virtual crack extension vector, A_c is the increase in crack area, δ_{ij} is the Kronecker delta, f_i are the components of the body force vector, t_i are the components of the surface tension vector and $W = \int_0^{\varepsilon_{ij}} \sigma_{ij}\,\mathrm{d}\varepsilon_{ij}$ is the total stress work density.

3. Finite-element model

The schematic diagram of the model is shown in Fig. 1. The finite-element model is made up of eight-node isoparametric plane-strain quadratic elements

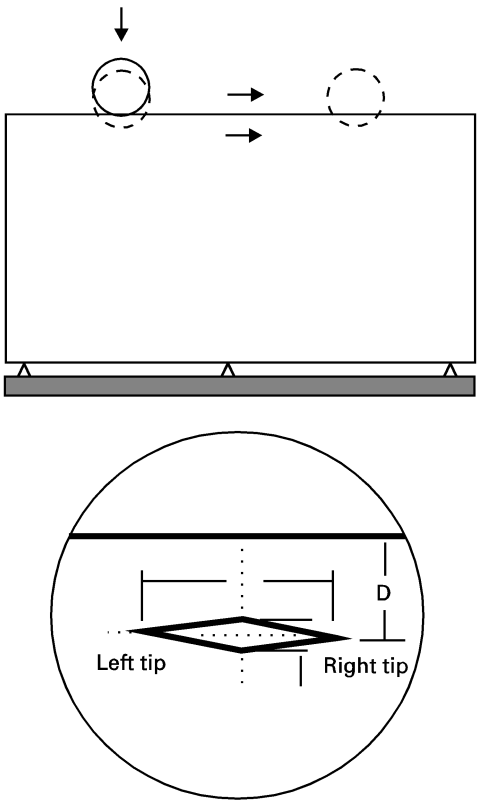

Figure 1 Schematic diagram of horizontal subsurface crack loading and boundary conditions.

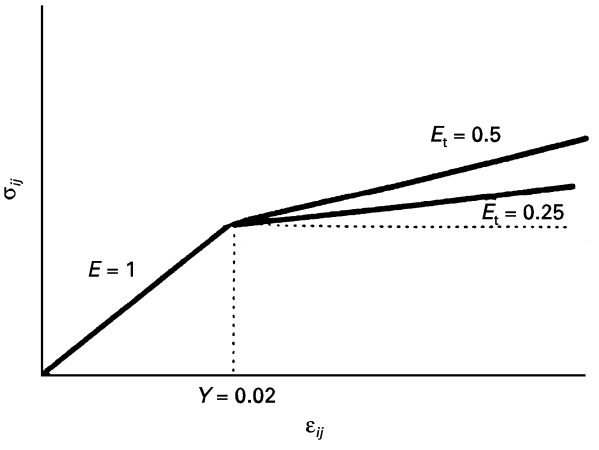

Figure 2 Elastic and elastic–plastic material properties (Poisson's ratio, $\mu = 0.2$).

capable of handling very large displacements with elasto-plastic properties (Fig. 2). The cylinder is assumed to be rigid and no body and/or inertia forces are included. During this isothermal process, the loading was considered to be monotonic and proportional, and the material properties were considered to be homogeneous. For the purpose of generality, the finite-element analysis was considered to be dimensionless, but there is no reason in principle why it cannot be related to our experimental studies.

As mentioned above, the constitutive model for the specimen material was based on a series of experimental microindentation tests which were reported in our previous publication [20]. Material response was

simplified to be similar to a bilinear elastic–plastic von Mises material.

4. Results and discussion

In sliding wear, several aspects of crack propagation are of interest:

1. where the sliding load is located when the subsurface crack starts to propagate;
2. which direction the crack should take;
3. how the crack's behaviour is affected by factors such as its depth, friction coefficient and crack geometry.

In our analysis we attempt to answer many of these issues.

Fig. 3 shows the variation in the J integral around the left crack tip with crack propagation angle, θ, for two different values of the elastic modulus E ($E = 1$ and $E = 3$). In the light of the theory proposed in our earlier paper [22], the left tip of this horizontal crack tends to grow in a direction of 170°, which is at an angle of 10° with respect to the horizontal (Fig. 4). As seen in Fig. 3, the elastic modulus of the material does not have any effect on the crack propagation angle. A similar variation of the J integral for the right tip is shown in Fig. 5. Again, the elastic modulus of the material does not affect the crack propagation direction, which is at 10° to the horizontal. The variation in the J integral values for the left and right horizontal crack tips indicates a propensity for the crack to propagate when the cylinder is sufficiently close to the crack tip.

Including friction between the indenter and the sliding surface does not seem to affect the prospective crack propagation direction for both the left and the right crack tips, as illustrated in Figs 6 and 7. The crack propagation directions for both crack tips are the same as shown in Fig. 4. This near-horizontal crack propagation direction is suggestive of a very high ratio of shear to normal stress. This is expected, as the crack is embedded in a compressive stress field and normal tensile stresses assisting the crack to open in mode I are absent. This behaviour is similar to the behaviour of a ductile sample subject to pure shear.

As mentioned earlier, the horizontal crack was modeled as a diamond-shaped crack with different height-to-width ratios, H/W. As indicated in Fig. 8,

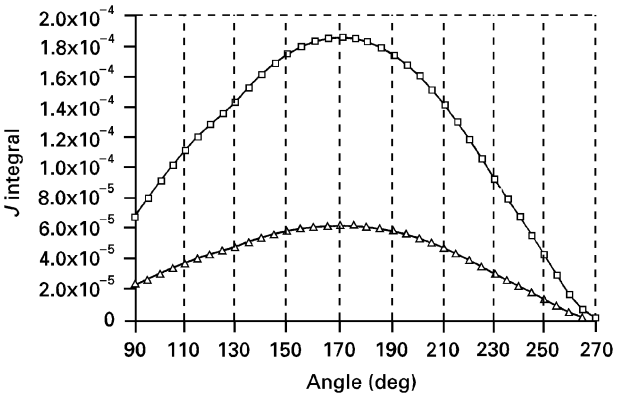

Figure 3 Graph of J integral versus left tip crack propagation angle, θ, under different elastic moduli. (△), $E = 1$; (□), $E = 3$.

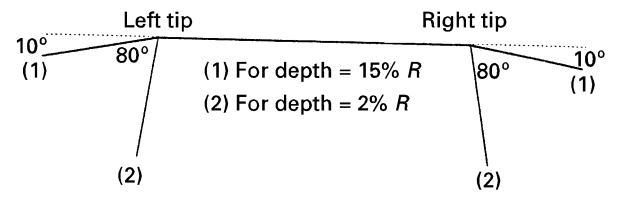

Figure 4 The range of crack propagation angles for different crack depths.

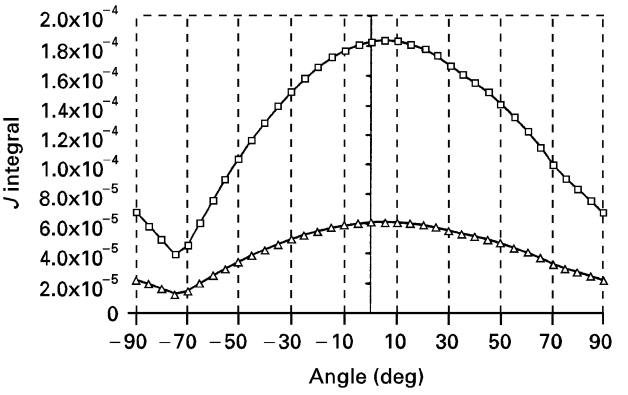

Figure 5 Graph of J integral versus right tip crack propagation angle, θ, under different elastic moduli. (△), $E = 1$; (□), $E = 3$.

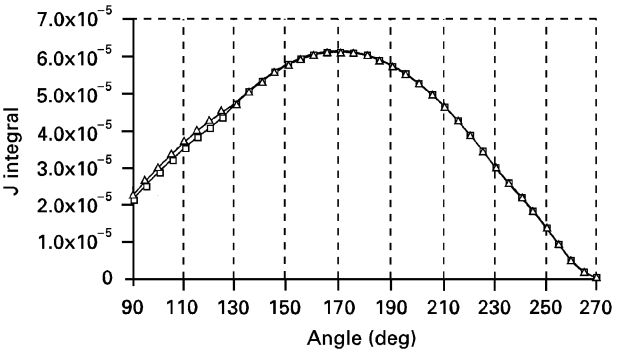

Figure 6 Graph of J integral versus left tip crack propagation angle, θ, under different contact friction coefficients. (△), $\mu = 0.18$; (□), $\mu = 0$.

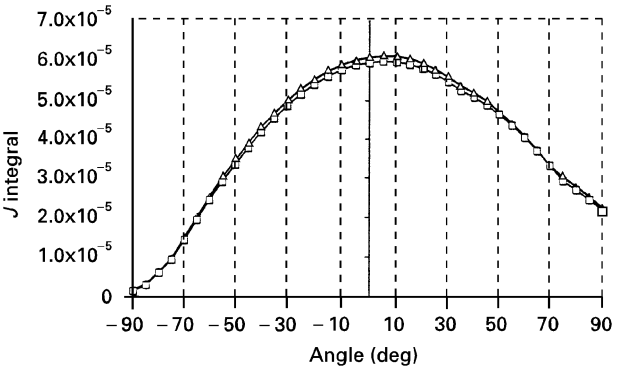

Figure 7 Graph of J integral versus right tip crack propagation angle, θ, under different contact friction coefficients. (△), $\mu = 0.18$; (□), $\mu = 0$.

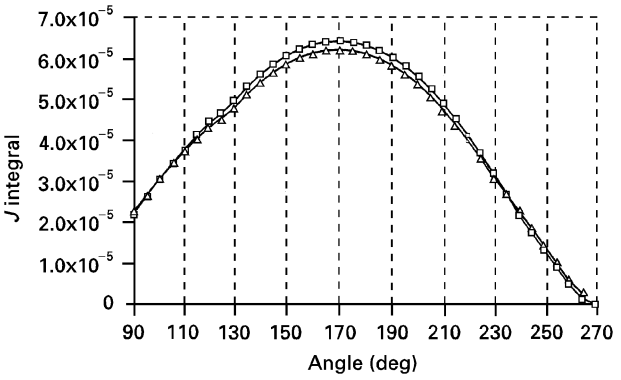

Figure 8 Graph of J integral versus left tip crack propagation angle, θ, under different crack geometric configurations. (△), $H/W = 0.1$; (□), $H/W = 1$.

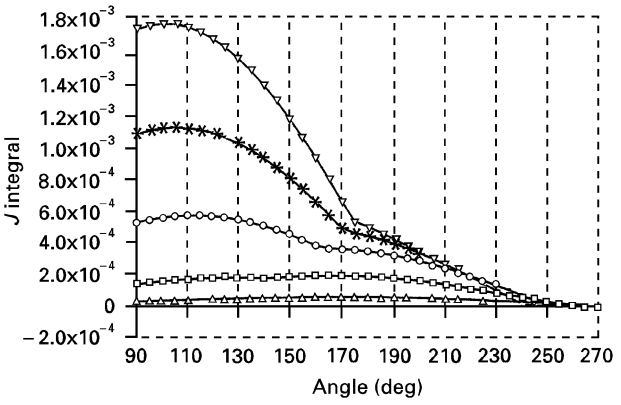

Figure 9 Graph of J integral versus left tip crack propagation angle, θ, under different crack tip depths. (△), $0.2R$; (∗), $0.1R$; (○), $0.05R$; (▽), $0.03R$; (□), $0.02R$.

increasing the height of the crack tends to increase the J integral values. This is suggestive of an increase in deformation in the vicinity of the left crack tip. However, H/W does not seem to affect the right crack tip field. The reason for this difference is not apparent.

An increase in the depth of crack location tends to decrease the left crack tip propagation direction. The angle of propagation for the left crack tip varies from 10° to 80° with respect to the horizontal as the location of the horizontal subsurface crack is decreased from 20% R to 2% R. The values for the right tip crack are the same as seen in Figs 9 and 10. This range of crack propagation angles is shown in Fig. 4. The lower values of the crack propagation angle are suggestive of pure shear. However, when the crack is located closer to the surface, the presence of a tensile stress field close to the contact area is probably responsible for the increase in crack propagation angle. Apart from a change in the crack propagation direction with depth of the crack, the tendency for crack propagation increases for cracks closer to the surface. This is evident from the sharp rise in the J integral values as the depth of crack is reduced from 20% R to 2% R.

The variation in the mode I and II stress intensity factors with any angle is represented in the following

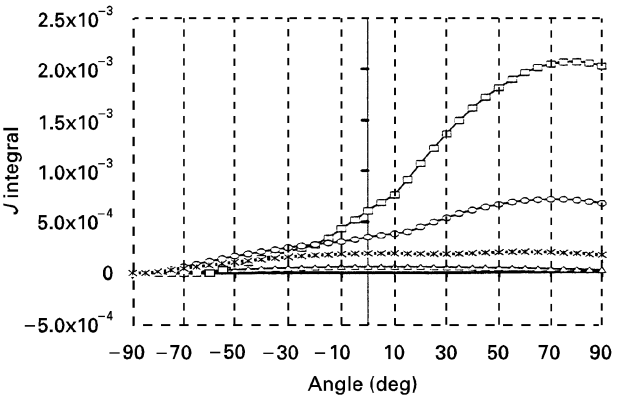

Figure 10 Graph of J integral versus right tip crack propagation angle, θ, under different crack tip depths. (△), $0.2R$; (∗), $0.1R$; (○), $0.05R$; (□), $0.02R$.

equations. The stress intensity factors along any angle, β, measured from the crack central line are given by

$$K_{\mathrm{I}}(\beta) = K_{\mathrm{I}}\cos^3\left(\frac{\beta}{2}\right) - 3K_{\mathrm{II}}\sin\left(\frac{\beta}{2}\right)\cos^2\left(\frac{\beta}{2}\right) \quad (4a)$$

$$K_{\mathrm{II}}(\beta) = K_{\mathrm{I}}\sin\left(\frac{\beta}{2}\right)\cos^2\left(\frac{\beta}{2}\right) - K_{\mathrm{II}}\cos\left(\frac{\beta}{2}\right)\left[1 - 3\sin^2\left(\frac{\beta}{2}\right)\right] \quad (4b)$$

These equations are obtained by assuming that the horizontal subsurface crack forms an infinitesimal kink at an angle θ from the crack plane [23]. The energy release rate, G, is thus a function of the crack propagation angle. For elastic materials, or materials with a low plastic-zone-to-crack-size ratio, this elastic energy release rate equals the J-integral value. Thus, the crack propagation direction would depend on the ratio of K_{I} to K_{II}. The above reasoning is mentioned only to justify the dependence of the J-integral values on the crack propagation angle. It needs to be emphasized that the values of these crack propagation directions obtained from these equations are different from those determined in the present study. This is probably on account of crack-tip plasticity which is not accounted for in Equations 4a and b, obtained using LEFM.

One other important factor that needs to be considered in attempting to compare the calculated crack propagation angles in the present study with experiment is the effect of crack-tip plasticity. This is illustrated in Fig. 11. Of particular interest in this figure is the sharp change in the predicted crack propagation direction of a material that has a plastic modulus of $0.25E$ compared with the pure elastic case. Also, the tendency of the crack to grow equally in directions symmetrical with respect to the crack plane increases with increase in plastic deformation.

In conclusion, the current study attempts to predict the crack propagation direction of a horizontal crack subjected to combined mode I and II loading. Also, the effect of crack-tip plasticity is accounted for in this analysis as the J-integral values are used as a measure of the crack propagation tendency.

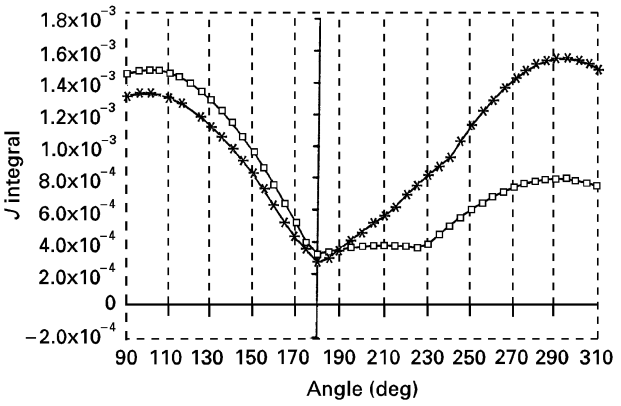

Figure 11 Graph of J integral versus left tip crack propagation angle, θ, under different plasticity ratios. (□), $E_t = 0$; (∗), $E_t = 0.25$.

5. Conclusions

J-integral values were used to estimate the crack propagation angle at the left and right tips of a horizontal subsurface crack. Based on this study, cracks closer to the surface have a tendency to propagate towards the vertical. As the location of the crack below the surface is increased, the cracks tend to propagate closer to the horizontal. This suggests that mode II type of loading dominates with increasing depth. Also, the J-integral values increase as the depth of crack location is decreased. Including friction between the indenter and the sliding surface does not affect the crack propagation direction. Introduction of crack-tip plasticity reduces the crack propagation angle of the left tip to 5° with respect to the horizontal. There was no change in crack propagation direction for the right tip.

The J-integral application has the advantage that it considers both modes (I and II) of crack propagation. Also, as J-integral values are used, the effect of crack tip plasticity is accounted for. Pin-on-disc experiments on polymeric restorative materials are currently being done to induce fatigue crack propagation in these materials. These will allow verification of predicted crack propagation directions.

Acknowledgement

This research is supported by National Institutes of Health Grant DE-09530.

References

1. R. KANEKO and E. HAMADA, *Wear* **162–164** (1993) 370.
2. K. FRIEDRICH, *J. Mater. Sci. Mater. Med.* **4** (1993) 266.
3. P. S. M. BARBOUR, D. C. BARTON and J. FISHER, *Wear* **181–183** (1995) 250.
4. B. J. BRISCOE, *Scripta Metall. Mater.* **24** (1990) 839.
5. N. P. SUH, *Wear* **25** (1973) 111.
6. J. R. FLEMING and N. P. SUH, *Wear* **44** (1977) 39.
7. A. R. ROSENFIELD, *Wear* **61** (1980) 125.
8. D. A. HILLS and D. W. ASHELBY, *Wear* **54** (1980) 321.
9. L. M. KEER, M.D. BRYANT and G. K. HARITOS, *J. Lubr. Technol.* **104** (1982) 347.
10. L. J. GHOSN, *J. Tribol.* **110** (1988) 408.
11. H. SALEHIZADEH and N. SAKA, *J. Tribol.* **114** (1992) 690.
12. A. R. ROSENFIELD, *Scripta Metall.* **24** (1990) 811.
13. H. C. SIN and N. P. SUH, *J. Appl. Mech.* **51** (1984) 317.
14. F. ERDOGAN and G. C. SIH, *J. Basic Eng.* **85** (1963) 519.
15. G. C. SIH, *Int. J. Fracture* **10** (1974) 305.
16. V. TIKARE and S. R. CHOI, *J. Amer. Ceram. Soc.* **76** (1993) 2265.
17. S. JAHANMIR, N. P. SUH and E. P. ABRAHAMSON, *Wear* **26** (1974) 235.
18. A. OTSUKA, K. MORI and T. MIYATA, *Fracture Mech.* **7** (1975) 429.
19. A. OTSUKA, K. MORI, T. OHSHIMA and S. TSYAMA, "Advances in fracture research, Proceedings of the Fifth International Conference on Fracture", Vol. 4, edited by D. François (Pergamon, Oxford, 1981) p. 1851.
20. K. SADEGHIPOUR, W. CHEN and G. BARAN, *J. Phys. D: Appl. Phys.* **27** (1994) 1300.
21. "Automatic dynamic incremental nonlinear analysis (ADINA), version 6.1" (ADINA R&D, Inc., Watertown, MA., 1992).
22. K. SADEGHIPOUR, K. BARAN, G. FU and S. JAYARAMAN (1997) submitted.
23. T. L. ANDERSON, "Fracture mechanics" (2nd Edn, 1995) p. 92.

Received 15 December 1995
and accepted 20 January 1997